Intercomparison of spectroradiometers and Sun photometers for the determination of the aerosol optical depth during the VELETA-2002 field campaign

V. Estellés,[1] M. P. Utrillas,[1] J. A. Martínez-Lozano,[1] A. Alcántara,[2] L. Alados-Arboledas,[2] F. J. Olmo,[2] J. Lorente,[3] X. de Cabo,[3] V. Cachorro,[4] H. Horvath,[5] A. Labajo,[6] M. Sorribas,[7] J. P. Díaz,[8] A. M. Díaz,[8] A. M. Silva,[9] T. Elías,[9] M. Pujadas,[10] J. A. Rodrigues,[11] J. Cañada,[12] and Y. García[13]

Received 5 April 2005; revised 18 January 2006; accepted 2 May 2006; published 15 September 2006.

[1] In July 2002 the VELETA-2002 field campaign was held in Sierra Nevada (Granada) in the south of Spain. The main objectives of this field campaign were the study of the influence of elevation and atmospheric aerosols on measured UV radiation. In the first stage of the field campaign, a common calibration and intercomparison between Licor-1800 spectroradiometers and Cimel-318 Sun photometers was performed in order to assess the quality of the measurements from the whole campaign. The intercomparison of the Licor spectroradiometers showed, for both direct and global irradiances, that when the comparisons were restricted to the visible part of the spectrum the deviations were within the instruments' nominal accuracies which allows us to rely on these instruments for measuring physical properties of aerosols at the different measurement stations. A simultaneous calibration on AOD data was performed for the Cimel-318 Sun photometers. When a common calibration and methodology was applied, the deviation was lowered to much less than 0.01 for AOD. At the same time an intercomparison has been made between the AOD values given by the spectroradiometers and the Sun photometers, with deviations obtained from 0.01 to 0.03 for the AOD in the visible range, depending on the channel. In the UVA range, the AOD uncertainty was estimated to be around 0.02 and 0.05 for Cimel and Licor respectively. In general the experimental differences were in agreement with this uncertainty estimation. In the UVB range the AOD measurements should not be used due to maximum instrumental uncertainties.

Citation: Estellés, V., et al. (2006), Intercomparison of spectroradiometers and Sun photometers for the determination of the aerosol optical depth during the VELETA-2002 field campaign, *J. Geophys. Res.*, *111*, D17207, doi:10.1029/2005JD006047.

1. Introduction

[2] Aerosol optical depth (AOD) and other related aerosol characteristics are routinely acquired throughout the world by means of well-established international networks such as the Aerosol Robotic Network [*Holben et al.*, 1998], Global Atmosphere Watch Programme (GAW) (available at http://www.pmodwrc.ch), or SKYNET (http://atmos.cr.chiba-u.ac.jp/aerosol/skynet/). These networks originated in the last decade and have been growing continuously with time, increasing the possibilities of long-term aerosol climatological studies in many sites across the world. These networks allow us to increase our knowledge of the role of aerosols in climate change, the effect of pollution on public health, or the validity of satellite retrieved products. Obviously, the uncertainties of the measurements are directly linked to the quality of the derived products. This problem is crucial when global radiative forcing by aerosols is to be determined [*Houghton et al.*, 2001], as the nature and quantity of atmospheric particulate matter are highly variable in space and time.

[3] Therefore the assessment and reduction of the uncertainty of the obtained aerosol optical parameters is a key

[1]Grupo de Radiación Solar, Universitat de València, València, Spain.
[2]Grupo de Física de la Atmósfera, Universidad de Granada, Granada, Spain.
[3]Departemento de Astronomía i Meteorología, Universitat de Barcelona, Barcelona, Spain.
[4]Grupo de Óptica Atmosférica, Universidad de Valladolid, Valladolid, Spain.
[5]Experimental Physics Institute, University of Vienna, Vienna, Austria.
[6]Instituto Nacional de Meteorología, Madrid, Spain.
[7]Estacion de Sondeos Atmosféricos de El Arenosillo, INTA, Huelva, Spain.
[8]Departemento de Física Básica, Universidad de La Laguna, Spain.
[9]Évora Geophysics Centre, University of Évora, Évora, Portugal.
[10]Departemento de Impacto Ambiental de la Energía, CIEMAT, Madrid, Spain.
[11]Departamento de Física, Universidade do Algarve, Faro, Portugal.
[12]Grupo de Radiación Solar, Universidad Politécnica de Valencia, Spain.
[13]Repsol YPF, Madrid, Spain.

0148-0227/06/2005JD006047

priority for the success of any of the already cited monitoring programs. As an example, the AERONET network has designed a carefully planned calibration program in order to maintain the uncertainty of the field instruments at a minimum [*Holben et al.*, 1998], at the same time that studies of the sensibility of the obtained retrievals have been published [*Dubovik et al.*, 2002]. The general scheme makes the whole program more reliable than other older programs, such as the Background Air Pollution Monitoring Network (BAPMoN) program which was discontinued in 1993 due to a lack of adequate data quality assurance [*World Meteorological Organization* (*WMO*), 1994].

[4] Occasional field campaigns also benefit from precalibrations and intercomparisons of their instruments, especially when nonfederated AERONET instruments are employed, as they usually come from a diversity of independent research groups that use different calibration strategies and aerosol parameter retrieval methodologies.

[5] In this paper we analyze the calibration and intercomparison issues for the VELETA 2002 field campaign, held in the Sierra Nevada Mountains (Granada) in southern Spain, from 8 to 22 July 2002. During the first week of the campaign, calibrations were obtained for all the instruments using both laboratory lamps and Langley calibrations. At the same time these instruments were intercompared. We present here the results relating to six Licor 1800 spectroradiometers and six Cimel CE318s. The analyzed results make reference to the calibration itself as well as the values that these instruments provide for the AOD within previous campaigns carried out by other authors [*Schmid et al.*, 1999; *Mitchell and Forgan*, 2003; *McArthur et al.*, 2003]. The importance of the AOD is that it can be considered the single most comprehensive variable to monitor the atmospheric aerosol load in the atmosphere [*Holben et al.*, 2001] and is a key parameter in remote sensing assessment of aerosol climatology across the world.

2. VELETA-2002 Campaign

[6] The VELETA-2002 field campaign was carried out in July 2002 in the area of Sierra Nevada (Spain) [*Alados-Arboledas et al.*, 2003]. This field campaign was designed to obtain experimental data about the effects of altitude and atmospheric aerosols on solar ultraviolet irradiance. For this purpose a set of radiometers and spectroradiometers were installed on and around the slopes of the Sierra Nevada Massif, from the coast to inland locations. The field stations included Motril, a coastal location at sea level, Pitres located on the south slope of the Sierra Nevada Massif, the Veleta Peak, Las Sabinas located on the north slope of the mountain range, and Armilla located in the valley near to the city of Granada.

[7] Figure 1 shows the locations of the stations. The vertical units represent elevation in meters above mean sea level. The principal feature of the locations is that they provide a strong altitudinal gradient considering that the horizontal separation from the Veleta Peak does not exceed 40 km. An additional feature is the proximity to the Mediterranean Sea and North Africa.

[8] At each station a Yankee UVB-1 radiometer, similar to those operated in the Spanish UVB radiation network [*Martínez-Lozano et al.*, 2002], was operated. Additionally, UV spectral measurements have been performed using different spectroradiometers including Brewer MK-IV, Bentham DM150, Optronic 754, Mechelle 900, and Oriel instruments. A complete coverage of the aerosol load at each station has been obtained from direct solar radiation extinction measurements obtained by LICOR Li1800 spectroradiometers equipped with collimator devices. In order to acquire additional information concerning the aerosol characteristics over each one of the stations, CIMEL CE318 robotic photometers were operated at four locations (excluding the Veleta Peak, 3398 m a.s.l.). In each of the measurement stations a meteorological station was also installed to continuously register the surface temperature, relative humidity, pressure and wind speed, and direction.

3. Instrumentation

[9] For the purposes of obtaining the AOD in the visible range six Licor 1800 spectroradiometers were used. In the following text these instruments are referred to as BCN (Univ. de Barcelona), UGR (Univ. de Granada), UV (Univ. de Valencia), VAL (Univ. de Valladolid), UPV (Univ. Politécnica de Valencia), and REP (Repsol YPF).

[10] The Licor 1800 spectroradiometer is equipped with a single monochromator that allows measurements in the 300–1100 nm range, with a full width at half maximum (FWHM) of approximately 6 nm and a wavelength step of 1 nm. The receiver in all the instruments is a Teflon diffuser, except in the VAL instrument in which it is a remote cosine sensor with a fiber optic probe. The main specifications of all the instruments used are listed in Table 1.

[11] Several papers have studied the uncertainty of the Licor 1800 spectroradiometer [*Riordan et al.*, 1989; *Nann and Riordan*, 1991; *Cachorro et al.*, 1998; *Martínez-Lozano et al.*, 2003]. The measurement error with these instruments depends on the spectral region considered. The greatest standard uncertainties (around 20%) correspond to the UVB range due primarily to the very broad slit function and single monochromator (i.e., stray light). In the visible and near-infrared regions (400–1000 nm) the standard uncertainty in the irradiance, governed by the calibration and measurement uncertainties, is 5% [*Martínez-Lozano et al.*, 2003], while in the range between 1000 and 1100 nm the standard uncertainty can increase significantly because of the sensitivity of the spectroradiometer to external temperature.

[12] For the direct irradiance measurements, collimators were used which had different FOVs (about 5°). The collimators were designed and constructed based on a design previously developed at the SERI (Solar Energy Research Institute), nowadays NREL (National Renewable Energy Laboratory) [*Cannon*, 1986]. In all cases, except the VAL instrument, in order to carry out the direct measurements a collimator was attached directly over the instruments' entrance. The measurements were made by mounting the complete spectroradiometer on a tripod with a three-axis ball-and-socket joint which, together with the incorporated Sun-pointing viewfinder, allowed the collimator to be pointed (see Figure 2). In the VAL case the collimator was directly adjusted over the remote cosine sensor, and it was this that was mounted on the tripod and ball-and-socket joint. The standard uncertainty associated with the circumsolar irradiance, which is typical of this type

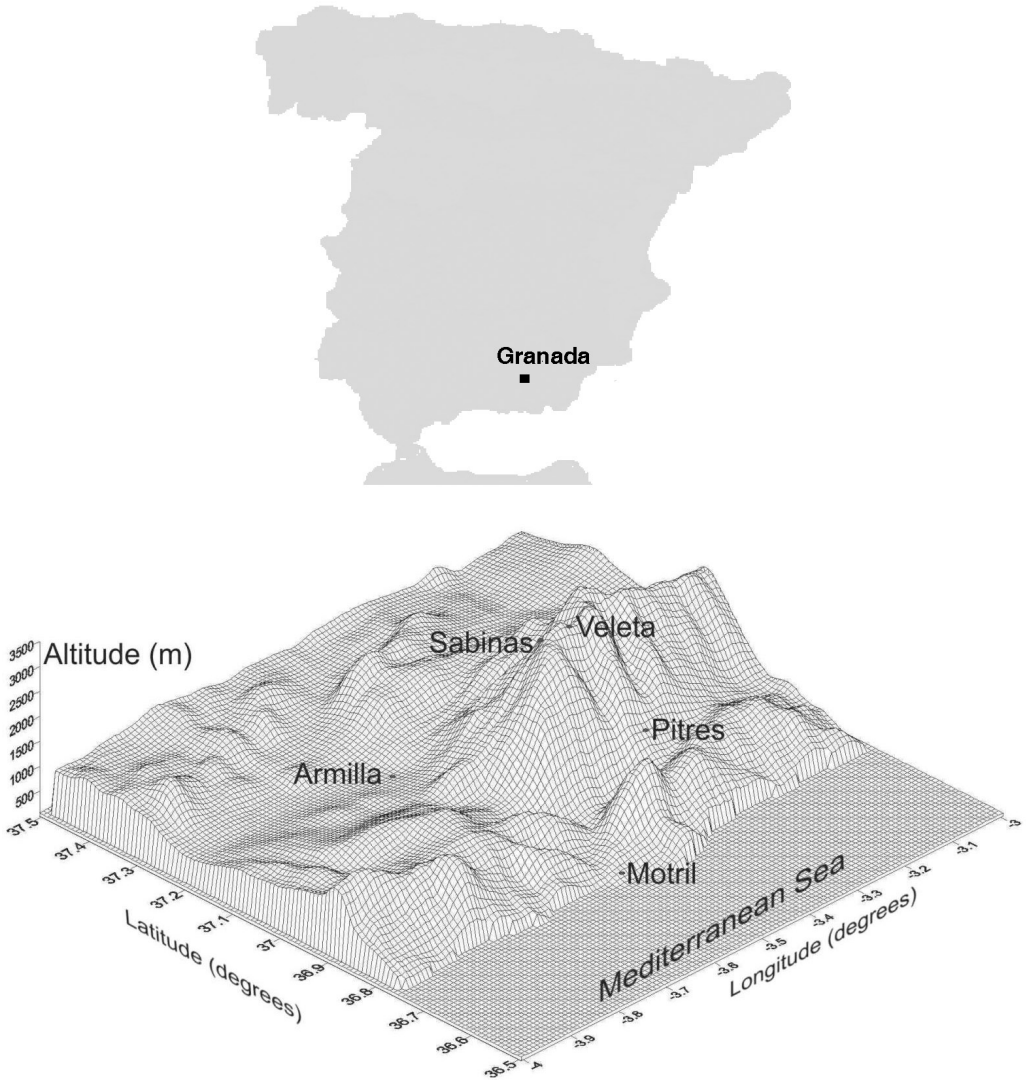

Figure 1. Location of the stations over the slice of the GTOPO DEM map from 36.5°N to 37.5°N and 3°W to 4°W. The horizontal coordinate system is decimal degrees of latitude and longitude referenced to WGS84.

of collimator, has been evaluated by *Martínez-Lozano et al.* [2003], concluding that, when measuring direct irradiance, the magnitude of the uncertainty is of the order of 0.2%.

[13] In addition to these spectroradiometers, six Cimel CE318 Sun photometers were also used. This automatic instrument is the standard Sun/sky photometer from the AERONET network [*Holben et al.*, 1998]. It consists of a sensor head, equipped with a filter wheel with eight interference filters, and a temperature sensor for the temperature correction of the signal for temperature dependent channels. A twin collimator tube (FOV 1.2°) is attached to the double windowed sensor head, in order to measure Sun and sky radiance with two different Si photodiodes. The scan of each series of eight channels lasts only 10 s, although three direct measurement cycles are taken 30 s apart for cloud discrimination and variability estimation. In Table 2 we show the filters used for the instruments used in the campaign. The letter labels attached to the serial number of the instruments stand for Grupo de Óptica Atmosférica (GOA) from University of Valladolid, National Aeronautic and Space Agency (NASA) that corresponds to AERONET instrument and was lent to the GOA for the campaign, Grupo de Radiación Solar de Valencia (GRSV) from University of Valencia, Centro de Geofísica de Évora

Table 1. Main Licor 1800 Specifications

Specification	Value
Entrance optic	PTFE (Teflon) cosine diffuser (except VAL, with remote cosine sensor with a fiber optic probe)
Quantity measured	Irradiance
Grating, groove mm^{-1}	800
Slit dimensions, nm	0.5
Filter trip point, nm	348, 418, 558, 678, 775, 938
Wavelength range, nm	300–1100
Resolution (FWHM), nm	6.25
Sampling step, nm	1
Collimator FOV	5.7 ° (except for VAL, 5.2 °)
Detector	Silicon Photodiode
Calibration Standard	1800-02L/ORL815

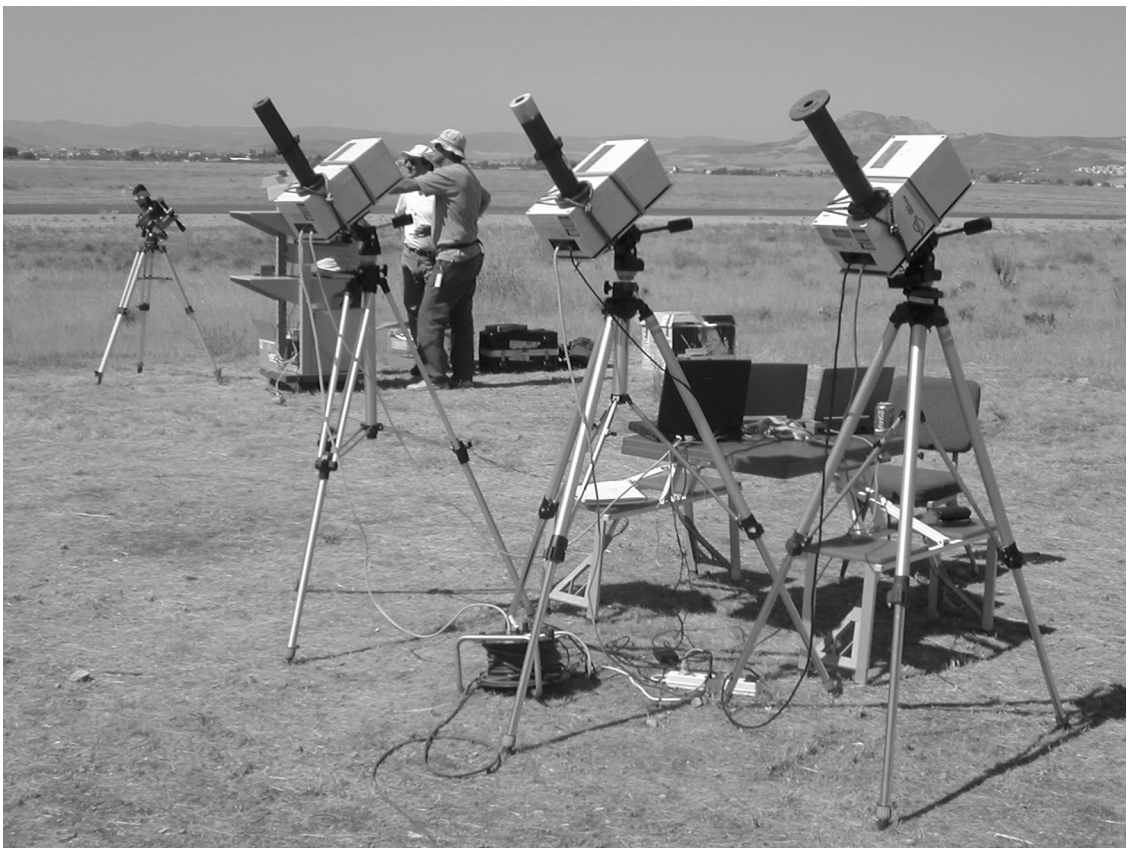

Figure 2. Several Licor 1800 spectroradiometers on tripods with three-axis ball-and-socket joints, which allow the collimators to be pointed.

(CGE), and Grupo de Física Atmosférica (GFAT) from University of Granada. For readability, we will refer to each instrument in this work by these labels, setting GFAT1 and GFAT2 for the two instruments from GFAT. In the table, the nominal wavelengths of the filters are presented. These nominal wavelengths will be employed in the text as channel denominators although the real wavelengths were used in the calculations. Signals for channel 1020 are corrected by its nominal temperature coefficient taken from [*Holben et al.*, 1998], except for the GRSV instrument whose experimental coefficients were determined at the Valencia University laboratories, giving similar results to those published by AERONET. The polarized channels for the three polarized instruments (GOA, GRSV, and CGE) were not used in this campaign.

4. Calibration

4.1. Licor 1800 Spectroradiometers

[14] The LICOR-1800s were calibrated using laboratory reference lamps and the Langley method. The reference lamps were those provided by the manufacturer in the calibration unit of each instrument. This calibration unit contains a 200 W tungsten halogen lamp inside of known irradiance and is calibrated in the factory with respect to a primary standard. Lamps of this type were provided by the Universities of Granada and Valencia.

[15] Previous to this calibration, all the instruments incorporated an original calibration file. Calibrations were performed using the Langley method to check the accuracy of these original calibrations [*Shaw*, 1983]. In order for the Langley calibration to be correct the atmospheric turbidity conditions must be stable. These conditions are verified more easily at high mountain sites, away from sources of aerosols and located above the greater concentration of aerosols in the mixing layers. Furthermore, at these altitudes the amount of atmosphere above the site is less and so is the air mass. For comparing the Langley extrapolation with the extraterrestrial irradiance spectrum, the proposed spectrum from *Gueymard* [2001] was chosen.

[16] In our case the Langley calibrations were carried out at the Sabinas station, at 2200 m a.s.l., between 8 and 9 July 2002. For 9 July a wider range of optical masses was obtained (between 1.1 and 3.8) which was more adequate for applying the Langley method. The Langley method was

Table 2. Measurements Channels From the Participant CIMEL Instruments[a]

Wavelengths, nm	340	380	440	500	670	870	940	1020
045 GOA	-	-	x	-	x	x	x	x
109 NASA	x	x	x	x	x	x	x	x
176 GRSV	-	-	x	-	x	x	x	x
248 CGE	-	-	x	-	x	x	x	x
307 GFAT1	x	x	x	-	x	x	x	x
394 GFAT2	x	x	x	-	x	x	x	x

[a]The serial number is accompanied by a label corresponding to the owner institution, as explained in the text. The nominal wavelengths in nanometers (column labels) are used in the text, although the real wavelengths were employed in the calculations.

Table 3. Average Values of the Deviations Between the Extraterrestrial Irradiance Value and the Value Obtained Through Langley Fitting for the Different Instruments Available on 9 July 2002[a]

MAD, %	BCN	UGR	REP	UPV	UV	VAL
340	56.6	5.4	1.2	3.0	1.0	6.3
380	27.2	3.8	3.8	1.9	3.9	3.0
440	29.0	0.8	2.1	0.4	5.1	5.0
670	8.7	0.5	0.03	0.8	1.3	4.1
870	0.4	1.6	0.4	2.4	1.8	2.7
1020	2.8	8.4	2.4	2.8	2.9	6.5

[a]Deviations are shown for the wavebands of the Cimel instruments.

applied to all the Licor instruments in the wavelength range from 340 to 1100 nm.

[17] In Table 3 the values of the relative MAD (Mean Absolute Difference) (in %) defined as

$$\mathrm{MAD} = \frac{1}{n}\sum_{i=1}^{n} |I_{\lambda 0} - I_{\lambda i}|, \quad (1)$$

are shown for each of the instruments that made measurements on 9 July, for the wavebands of the Cimel instruments. In this expression, $I_{\lambda 0}$ and $I_{\lambda i}$ refer to the calibration coefficients from the extraterrestrial spectrum given by *Gueymard* [2001] and the Langley derived coefficients, respectively. The MAD was employed instead of the standard deviation because the Gaussian shape of the differences distribution is not a priori satisfied. As can be seen, the deviations in the Langley fits against the extraterrestrial irradiance in the visible range were less than the given precision of the instruments, except in the case of the BCN instrument. This instrument, owing to technical problems at the beginning of the morning measured a very small range of optical masses for which the results of the Langley method were not valid. Thus for the calibration of this instrument the coefficients derived from the laboratory reference lamp of the Valencia University were used.

4.2. Cimel CE318 Sun Photometers

4.2.1. Simultaneous Langley Calibration

[18] Table 4 shows the measurement sites of the different Cimel instruments during the first phase of the campaign. For the Langley calibration of the instruments, mornings from 8 to 11 July were devoted to simultaneously measuring direct irradiance at Las Sabinas site, 2200 m.a.s.l. The morning of 9 July was chosen as the most stable after a careful analysis of the data sets, and therefore preliminary calculations were made with these calibration factors, except for the failed GFAT2 instrument that used a transferred calibration from GFAT1. When we took the calibration coefficients obtained in this way for the AERONET instrument, and compare them to the coefficients obtained from AERONET for this Sun photometer, the results in Table 5 were found. In this table we show the deviation, as the difference between the two values divided by the AERONET value, written in percentage. The correlation coefficient (R) and the percentual standard deviation of the fit (σ) written in terms of V, are also presented. Moreover, the whole available air mass range for this instrument has been used (from 1.3 to 3.5), that is narrower than the other instruments air mass ranges (1.3 to 5.0 or 6.0) due to differences in the deployment time.

[19] A sensitivity study of the calibration constants with the air mass range was previously made for this day. Two reasons are given: first, a robust calibration should be independent of slight changes on the plot air mass range [*Kuester et al.*, 2003]. Second, if the instruments have different available air mass ranges, the calibration cannot be dependent on them. On the contrary, the calibration could not be homogeneous, in spite of their simultaneity. These preliminary results showed the calibration to be only dependent by 0–1% except for the UV channels. The NASA instrument complete air mass range (up to 3.5) gave good results in comparison with the AERONET provided calibration, except for 340 and 380 nm. For these lowest wavelengths, a reduced air mass range gave better results, with a maximum air mass of 2 [*Slusser et al.*, 2000]. With this reduced range, the deviations for 340 and 380 nm were found to be 1.8 and 0.11%. A reason to this calibration dependence on the air mass could be related to a higher diffuse and straylight contribution for higher air masses [*Slusser et al.*, 2000]. Calibration of UV filters remains in any case more problematic than visible wavelengths, as the AERONET uncertainty is also higher at this band.

[20] In spite of the relatively low deviations found for the retrieved calibration coefficients, some problems remained. First, not all the mornings at Las Sabinas were stable enough. After a careful analysis of the available data was made, only one Langley plot was performed. Usually, several Langley plots are recommended to be performed for an adequate uncertainty estimation. Second, not all the instruments were available all four days. Third, each instrument started to measure at slightly different times, a few

Table 4. Location of the Cimel Instruments During the First Phase of the Campaign[a]

	8 Jul		9 Jul		10 Jul		11 Jul	
Instrument	m	a	m	a	m	a	m	a
GOA (045)	X	O	X	+	X		+	+
NASA (109)		O	X	+	X	+	+	+
GRSV (176)	X	O	X	+	X	+	+	+
GFAT1 (307)	X	O	X	+	X	+	+	+
GFAT2 (394)	X	O	X	+	X	+	+	+
CGE (248)	X	O	X	+	X	+	+	+

[a]Here the crosses represent the Las Sabinas site, the circle is the Lamp calibration, and the plus symbol is the Armilla site. Here m is morning and a is afternoon.

Table 5. Deviation Between AERONET Provided Calibration Coefficients and Our Retrieved Coefficients by Langley Plot Fit for 9 July, for NASA Instrument, When the Whole Available Air Mass Range Was Used[a]

λ, nm	σ, %	R	Deviation, %
340	0.40	0.998	3.8
380	0.39	0.999	1.9
440	0.69	0.996	0.6
500	0.26	0.999	0.3
670	0.29	0.992	0.9
870	0.17	0.98	0.05
1020	0.15	0.98	0.6

[a]R stands for the correlation coefficient and σ for the standard deviation of the fit (in percentage).

Table 6. Retrieved Calibration Coefficients[a]

Wavelength, nm	V_0	Standard Error of the Mean	% Error
340	21024.29	244.46	1.16
380	33057.31	329.16	1.00
440	3971.52	27.83	0.70
670	9508.00	37.51	0.39
870	4936.30	25.72	0.52
1020	3526.47	19.56	0.55

[a]Average value and standard error of the mean.

minutes, due to deployment delays (the site was not supervised and the instruments were daily brought from the Armilla site; at this time of the year, delays of few minutes easily lead to no negligible differences in air mass), therefore different air mass ranges were available for each instrument. Fourth, one of the Sun photometers (GFAT2) failed due to robot and filter problems. Therefore this procedure could not be generalized for all the instruments and some of them were not well calibrated or their calibration could not be verified.

[21] In addition, the procedure explained above accepts the AERONET supplied calibration as a reference calibration. The main question that arose at this point is related to its reliability as a reference instrument. As this instrument has been only calibrated by comparison with a true reference Sun photometer in Goddard Space Flight Center (GSFC), the calibration could possibly be degraded in such a way that the uncertainty of our instruments could be unexpectedly high. If we considered the reference instruments in AERONET to have an uncertainty in their calibration coefficients of around 0.25–0.5% in the visible range and 0.5–2.0% in the UV band [*Holben et al.*, 1998] and we accept that this uncertainty could be even doubled in the transfer process when collocated instruments are compared under clear sky conditions [*Pietras et al.*, 2001], we would conclude that the field instruments can easily reach a calibration uncertainty of 1–2% [*Campanelli et al.*, 2004], higher for UV wavelengths. The uncertainty in our instruments will be higher after a calibration transfer from this AERONET field instrument. Even higher errors could appear in cases of spurious problems in the AERONET instrument. Errors in the AERONET calibration coefficients have been previously reported by other authors [*Cachorro et al.*, 2004].

4.2.2. Master Langley Calibration and its Transfer to the Other Sun Photometers

[22] To provide a workable reference in this situation, a master instrument was selected amongst our available Sun photometers. The GFAT1 instrument was chosen, mainly because it was deployed at the Las Sabinas site, the highest available CIMEL site in our field campaign (over 2200 m.a.s.l.). Moreover, this instrument measures at all the wavelengths used in the field campaign and it showed no technical problems in the intercalibration stage compared under good conditions.

[23] The Langley procedure was applied to the available morning and afternoon measurements. The results shown here correspond to Langley plots computed on the total optical depth without separation of the contribution of the different attenuators at each waveband [*Mitchell and Forgan*, 2003; *Schmid and Wehrli*, 1995; *Kuester et al.*, 2003]. In doing this we had to bear in mind that the filters of the instruments, excluding the one at 936 nm, correspond to bands of low gaseous absorption. In this sense the use of different air masses for each atmospheric component provided results that are only slightly different than those obtained assuming the same air mass for all of them. Thus for good quality Langleys the discrepancies between the calibration coefficients obtained by both methods were less than 0.1% [*Alcántara et al.*, 2004].

[24] From the available Langley plots retrieved using morning and afternoon data we have selected those with lower aerosol optical depth (AOD at 670 nm less than 0.09). Finally, three morning and one afternoon Langley plots were selected. For the selected cases the correlation coefficients were always greater than 0.995. The calibration coefficients applied were the averages of these four cases. In all circumstances the selected Langley plots presented calibration coefficients for all the channels that differed from the average value by less than 3 times the standard deviation. Table 6 shows the retrieved calibration coefficients, including the average value and the standard error of the mean. The last column shows this error in percent. It is important to say that this column divided by 100 gives an estimate of the maximum error associated to the aerosol optical depth in each channel. It is evident that the errors were close to 0.01 with better results in the longer wavelengths, results that were in the range of those of AERONET [*Holben et al.*, 1998; *Eck et al.*, 1999]. It must be said that during the periods used for the Langley calibration the total columnar ozone do not vary more than 5% according to the analyses of the measurements performed by a Brewer MKIII at Armilla main station.

[25] Once the calibration was performed for this instrument, the coefficients were transferred to the other Cimel Sun photometers. For the transfer only data that met several criteria were accepted. First, the air mass had to be lower than 3.5. Second, stable conditions had to be met, to avoid rapid changes in the optical depth that could have led to hidden trends in the coefficient ratios. Third, measurements had to be simultaneous or within 5 s difference.

[26] After these criteria were met, a 3σ filter was applied to the obtained ratio datasets, and a mean value and standard deviation were calculated for each instrument and wavelength. The uncertainty for the transferred calibration coefficients was estimated to be the sum of the uncertainty of the reference coefficients and the standard deviation from the ratio data set. This estimated uncertainty was 1–2%, depending on wavelength and coincident with AERONET field instruments calibration uncertainties [*Campanelli et al.*, 2004].

[27] The deviation shown in Table 7 refers to the comparison between the AERONET supplied calibration coefficients for 109 and the 109 new coefficients resulting from the GFAT1 transfer. As can be seen in this table, the percent differences were not high in most cases, taking into account that the nominal uncertainty for calibration coefficients from AERONET field instruments is around 1–2%. Therefore in general, we can consider our procedure to have been very consistent in comparison with the AERONET calibration.

[28] The exceptions were the 340 nm and 670 nm channels. A possible reason for such a high deviation for channel 340 nm could be related to the air mass range

Table 7. Deviation Between AERONET Provided Calibration Coefficients and Our Transferred Coefficients From GFAT1 Instrument, for 109 Unit

λ, nm	Deviation, %
340	4.0
380	0.4
440	0.5
670	1.6
870	0.4
936	0.8
1020	0.3

employed in the Langley plot. As mentioned before, in the work of *Holben et al.* [1998] it is stated that the UV channels have a higher uncertainty in their calibration coefficients even for the master instruments (0.5–2.0%). The optimum air mass range for performing a Langley plot in the UV range is not completely agreed [*Slusser et al.*, 2000; *Morys et al.*, 2001] (http://aeronet.gsfc.nasa.gov/) leaving an inherent difficulty in calibration and therefore a higher resulting uncertainty. However, for channel 670 nm, the problem probably comes (at least in part) from the AERONET calibration. Two reasons were found: on one hand, the results of another Langley calibration performed on the GFAT instruments after the end of the campaign confirmed the calibration coefficients obtained within the field campaign; and on the other hand, the aerosol optical depth spectra became smoother when our retrieved value was used instead of the AERONET supplied coefficients. The slight difference on central wavelengths from NASA and GFAT1 filters in the cross-calibration stage [*Pietras et al.*, 2001] would not explain this deviation.

5. Intercomparison

5.1. Licors 1800 Intercomparison

[29] The intercomparisons between the Licor 1800s were performed in Armilla during 10 and 11 July including both global and direct irradiances. Measurements were taken from 0600 to 1800 UTC every 15 min, alternating global and direct irradiance measurements. Each scan has a length of 27 s. As an indicator of the goodness of the comparison the MAD (in %) was used. We analyzed first the spectral measurement series using the original calibration file of each instrument, i.e., the last calibration available for each instrument before the field campaign, obtained routinely by the instrument owners. Figure 3 shows the spectral global irradiance measurements corresponding to 10 and 11 July at solar noon. In Figure 4 the average values of MAD (in %) are summarized for the visible range (400–670 nm) corresponding to the relative values for each day, for each pair of instruments. These average values refer to the average MAD corresponding to the 271 spectral values of all the measurements available each day. This type of analysis was chosen for instrument pairs instead of taking the average value of the weighted results as a reference as is usual in this sort of intercomparison [*Labajo et al.*, 2004] in order to better detect possible malfunction in specific instruments. It should be noted that no measurement series has been excluded, having included all the series taken from 0600 solar time to 1800 solar time, despite the deviations detected in a previous work in relation to the global irradiance measurements for zenith angles greater than 60° [*Martínez-Lozano et al.*, 2003]. Table 8 summarizes the average MAD values (in %) for each of the instrument pairs for the wavebands of the Cimel instruments. From Table 8 it can be seen that all pairs of instruments showed acceptable results, around 5% which is the instruments' uncertainty, except those pairs including the VAL instrument for wavelengths lower that 670 nm. It should be remembered that this instrument was the only one that used a different measurement procedure to the rest with a fiber optic connected to a remote cosine sensor mounted over the optical window.

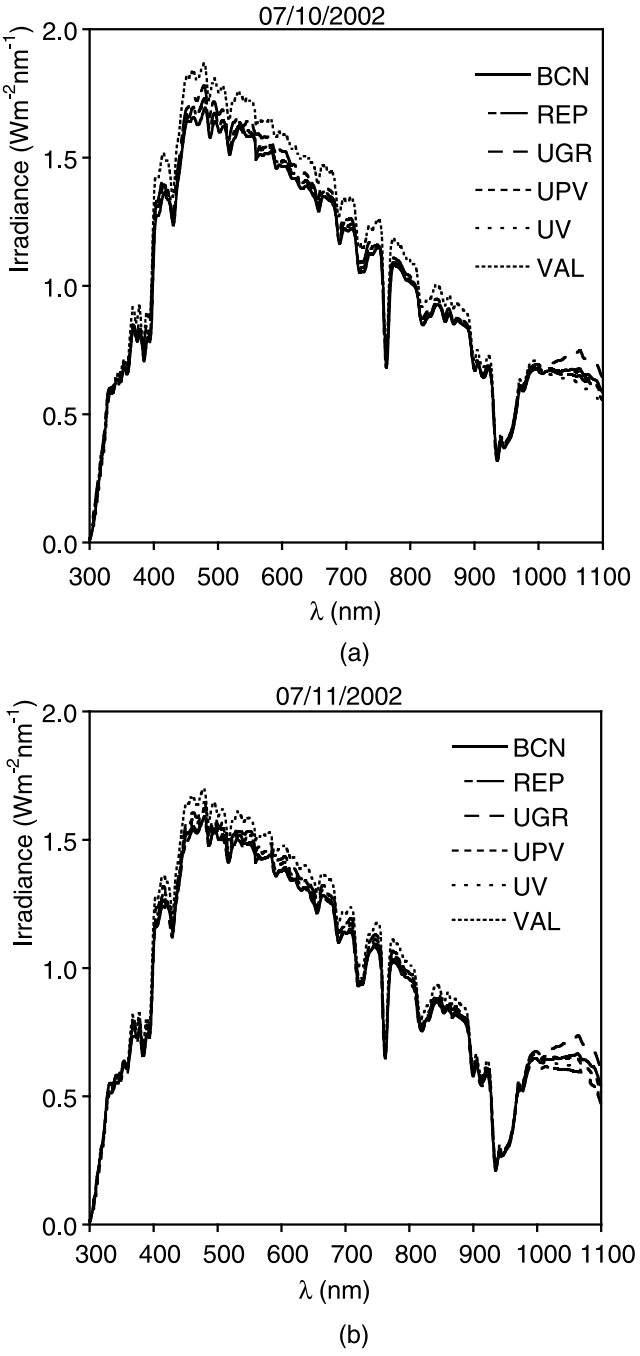

Figure 3. Global spectral irradiance measurements taken with the different Licor 1800s at Armilla at solar noon.

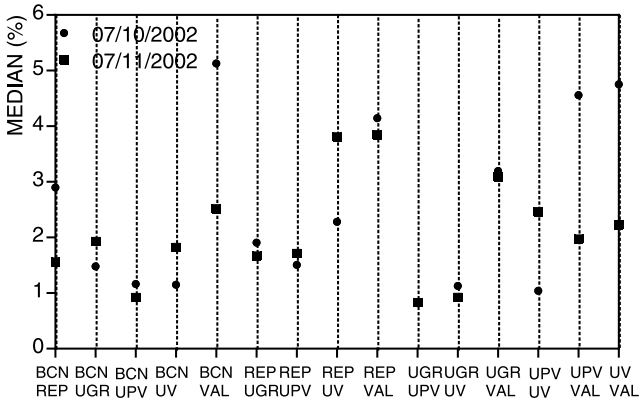

Figure 4. Average MAD values (in %), for the visible range (400–670 nm), corresponding to all the values of global irradiance relative to each day for each pair of Licor 1800 instruments in Armilla.

[30] A similar analysis to the previous one has been carried out for the measurements of direct irradiance. Figure 5 shows the spectral direct irradiance measurements at solar noon corresponding to 10 and 11 July, respectively. Figure 6 summarizes the average MAD values (in %) for the visible range (400–670 nm) corresponding to all the relative values for each day, for each pair of instruments. It should be noted that the UPV instrument did not measure direct irradiance on 11 July due to a software problem. In Table 8 the average MAD values (in %) are summarized for each instrument pair for the wavebands of the Cimel instruments.

[31] From Table 8 it can be seen that in the case of the BCN instrument the errors were a little higher than the rest, whilst those involving comparisons with the VAL instrument gave errors notably greater than the rest of the instruments. The UGR, REP, UPV, and UV instruments presented very similar and highly accurate results.

[32] All the Licor instruments were recalibrated by the Langley plot method, except BCN and VAL units, which calibration was carried out with the LICOR 1800-02 lamp from the University of Valencia. The BCN and VAL were the only two instrument not calibrated right before the field campaign. After applying the new calibration, the previous analysis was repeated, giving the results shown in Table 9. In this case, for the direct irradiance, all the deviations stayed below 3% in the visible range, the established error for this type of measurement for these instruments [*Martínez-Lozano et al.*, 2003]. Table 8 allows us to get information on the calibration stability of Licor instruments, particularly in the UV range.

[33] This allows us to affirm that the Licors are adequate instruments for measuring direct solar irradiance, and the results that they give are comparable, even when the optics of the receiver and the FOV of the collimator are different. For global irradiance the results were somewhat similar, in all cases the deviation was less than 5% (the established precision of these instruments for these measurements).

5.2. Cimel CE318 Intercomparison

[34] The intercomparison of the Cimel 318 instruments was carried out based on the measurements they provided of the AOD. The determination of AOD is affected by a series of factors such as: the calibration, the optical mass, the Rayleigh dispersion model, and the absorption coefficients of O_3, H_2O, and NO_2. A preliminary comparison of AOD was made after the initial calibration was completed, as discussed in section 4.2.1. As the instruments were operated individually by the different research groups, several differences were present in the methodology employed for calculating AOD. AERONET methodology can be found elsewhere [*Holben et al.*, 1998]. In Table 10 the main differences in the other computation methodologies are presented. Here we show the results in order to point out the importance of getting a common methodology when data from different instruments are being used.

[35] For the quantitative comparison, several statistical indicators were used. These were the root mean squared deviation (RMSD), the mean bias deviation (MBD), and the standard deviation of the differences (STD).

$$\mathrm{RMSD} = \sqrt{\frac{1}{n}\sum_{i=1}^{n}(\tau_0 - \tau_1)^2}, \qquad (2)$$

Table 8. Average MAD Values, %, Corresponding to Direct and Global Irradiance for the 2 Days of the Intercomparison, for Each Pair of Instruments, in the Wavebands of the Cimel Instruments[a]

	GLOBAL						DIRECT					
MAD, %	340	380	440	670	870	1020	340	380	440	670	870	1020
BCN-REP	33.8	26.7	8.9	2.7	2.6	1.0	32.0	25.0	7.2	0.8	1.4	1.6
BCN-UGR	31.1	28.8	7.4	2.4	2.1	4.7	32.8	28.4	8.4	2.3	2.2	3.5
BCN-UPV	31.1	28.5	8.2	1.4	1.7	2.0	31.9	28.0	7.9	1.1	1.7	1.7
BCN-UV	28.0	27.7	5.5	1.4	1.7	4.3	27.4	27.3	6.6	1.4	1.2	3.1
BCN-VAL	27.9	30.1	15.8	7.6	4.3	3.6	29.1	31.2	15.8	8.4	4.5	2.7
REP-UGR	3.0	1.9	2.1	1.5	1.0	5.8	1.6	3.3	3.3	1.6	1.1	7.5
REP-UPV	2.4	1.2	1.0	1.6	1.0	1.9	1.8	2.4	2.4	0.6	0.9	2.9
REP-UV	5.2	1.8	2.9	2.5	3.0	1.8	3.9	3.3	3.3	1.0	1.5	1.4
REP-VAL	3.1	6.9	10.3	8.1	4.7	4.3	2.5	7.0	9.0	8.3	3.7	4.8
UGR-UPV	1.4	1.1	1.1	0.6	0.6	3.7	0.7	0.5	0.5	1.3	1.4	4.8
UGR-UV	3.4	1.0	1.0	1.5	2.3	8.1	4.3	1.0	1.0	1.7	2.1	8.1
UGR-VAL	3.0	4.7	12.0	9.5	5.6	2.2	3.6	3.3	8.3	6.9	2.9	2.5
UPV-UV	2.1	1.3	1.7	1.5	3.0	4.9	2.8	1.4	1.4	1.2	1.4	3.8
UPV-VAL	3.7	5.6	10.2	8.9	5.1	2.7	1.8	6.0	10.3	9.4	5.5	3.2
UV-VAL	2.9	5.6	13.1	10.4	7.9	7.2	2.6	5.0	10.0	8.5	5.1	6.8

[a]Analysis performed using the original calibration file of each instrument.

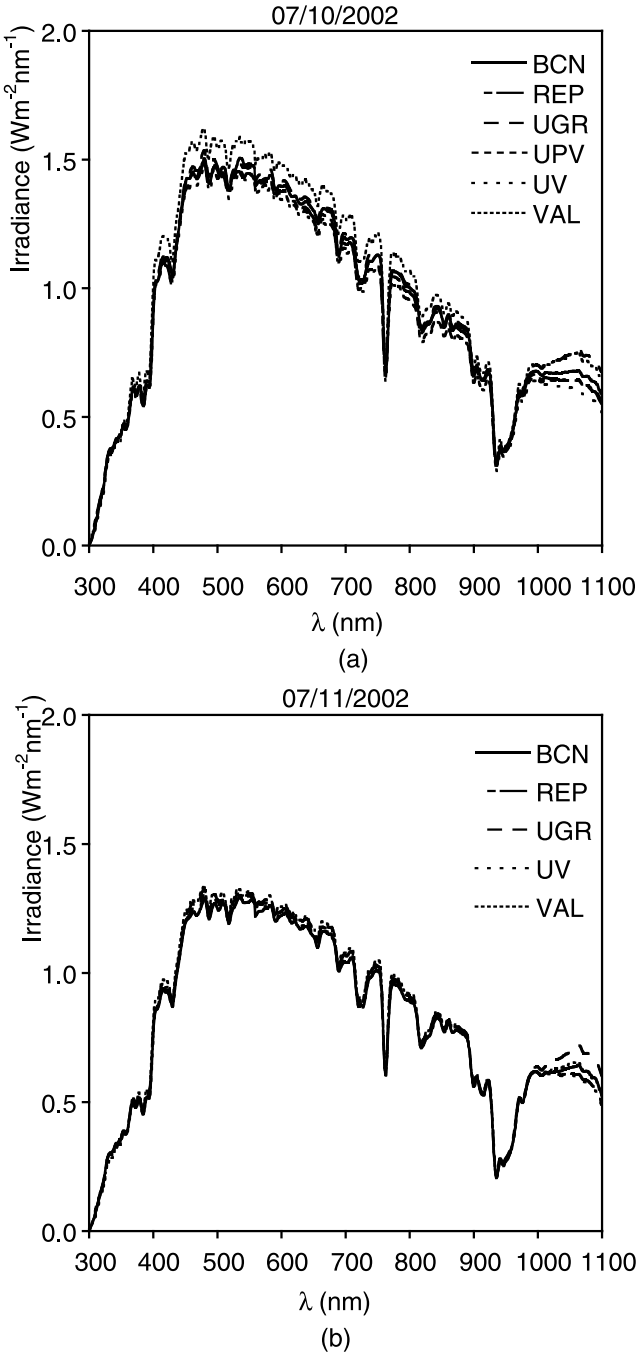

Figure 5. Direct spectral irradiance measurements taken with the different Licor 1800s in Armilla at solar noon.

$$\mathrm{MBD} = \frac{1}{n}\sum_{i=1}^{n}(\tau_0 - \tau_i), \tag{3}$$

$$\mathrm{STD} = \sqrt{\frac{1}{n}\sum_{i=1}^{n}\left(\delta_i - \overline{\delta}\right)^2}, \tag{4}$$

where δ stands for the difference between two simultaneous values of AOD for the reference (subscript 0) and field instrument (subscript i), and $\overline{\delta}$ coincides with the mean bias deviation. We considered two measurements to be simultaneous when they differ by less than 1 min.

[36] Figure 7 presents the comparison between the AOD for 440 nm, evaluated using each instrument with its own methodology during the intercomparison phase of the field campaign. The error bars, obtained through error propagation, are not plotted for the purpose of clarity. The data for AERONET Sun photometers was downloaded from the website (http://aeronet.gsfc.nasa.gov/). In Table 11, the several statistical indicators between the temporal series of AOD for the different instruments and for the master instrument (GFAT1) are given.

[37] As can be seen in Table 11, the RMSD between any pair of instruments was typically less than 0.02 for AOD, except for a few wavelengths where this deviation was slightly higher. An exception was the 340 nm channel for instrument GFAT2, but this instrument was seen to fail with the 340 nm filter. The nominal uncertainty for the field instruments of AERONET is stated to be around 0.01–0.02 for AOD depending on the wavelength [*Eck et al.*, 1999]. Therefore for most of the instruments and wavelengths our deviations were of the order of this uncertainty.

[38] So far we have compared the performance of the different methodologies for AOD, giving acceptable results. However, for the analysis of the measurements at the different sites, we needed to reduce the instrumental and methodological deviation, in order to better assess the differences of the aerosol characteristics between sites. At this point a common methodology was chosen including the common calibration introduced in section 4.2.2. For simplicity a single optical air mass, proposed by *Kasten and Young* [1989] was taken for all components. The equations for the solar position were those of *Blanco-Muriel et al.* [2001] and the zenith angle refraction correction given by *Michalsky* [1988] and generalized of the SMARTS 2.8 model [*Gueymard*, 2001] was used. To calculate the molecular scattering the algorithm of *Bodhaine et al* [1999] was used.

[39] The value for pressure was taken from the values provided by the INM at each station. To obtain ozone optical depth we adopted the absorption coefficients of *Anderson and Mauersberger* [1992], which are convoluted to the Gaussian transmissivity profile of each filter (grid

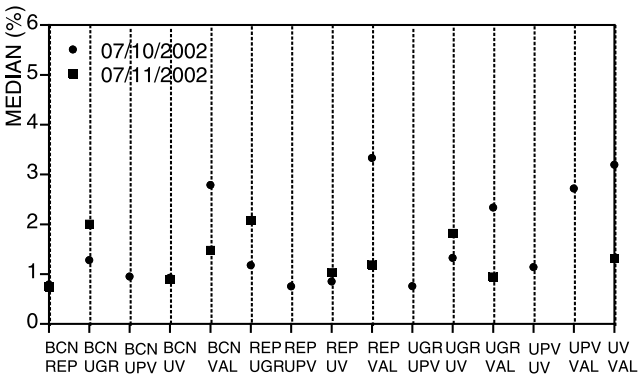

Figure 6. Average MAD values (in %) for the visible range (400–670 nm), corresponding to the values of direct irradiance relative to each day for each pair of Licor 1800 instruments in Armilla.

Table 9. Average MAD Values, %, Corresponding to Direct and Global Irradiance for the 2 Days of the Intercomparison, for Each Pair of Instruments, in the Wavebands of the Cimel Instruments[a]

	GLOBAL						DIRECT					
MAD, %	340	380	440	670	870	1020	340	380	440	670	870	1020
BCN-REP	1.9	1.8	1.8	1.7	1.9	2.2	1.3	3.4	3.4	0.7	0.8	2.2
BCN-UGR	1.5	1.4	1.3	1.3	1.3	3.4	0.6	0.8	0.8	1.4	1.5	5.4
BCN-UPV	1.8	0.5	1.3	0.8	1.5	1.4	1.3	0.6	0.6	0.6	1.0	1.6
BCN-UV	3.8	1.7	1.5	1.2	1.7	3.3	4.5	1.3	1.3	0.9	0.9	3.1
BCN-VAL	3.4	3.4	2.8	2.6	2.0	2.6	4.5	2.6	2.6	1.5	1.5	0.8
REP-UGR	2.0	1.8	2.1	1.5	0.9	5.0	1.4	3.0	3.0	1.4	1.0	7.0
REP-UPV	2.3	1.2	0.9	1.6	0.9	1.8	1.8	2.4	2.4	0.6	0.9	2.9
REP-UV	5.0	1.4	2.4	2.5	2.5	1.8	3.9	3.3	3.0	1.0	1.5	1.4
REP-VAL	2.7	2.9	1.3	3.5	2.8	2.6	3.4	1.5	1.5	2.3	1.8	3.1
UGR-UPV	1.4	1.1	1.1	0.6	0.6	3.5	0.7	0.5	0.5	1.2	1.4	4.0
UGR-UV	3.0	1.0	0.9	1.5	2.3	6.1	4.0	1.0	1.0	1.5	2.1	7.1
UGR-VAL	2.4	2.7	3.5	2.2	2.6	3.7	4.4	2.5	2.5	1.2	1.1	4.0
UPV-UV	2.1	1.3	1.7	1.5	2.6	4.9	2.8	1.4	1.4	1.2	1.2	3.8
UPV-VAL	3.0	2.8	2.3	2.3	2.5	2.2	1.6	1.5	1.5	2.8	2.9	1.4
UV-VAL	1.4	1.7	5.2	3.7	4.7	5.3	1.5	1.3	1.3	2.7	2.9	4.9

[a]Analysis performed using the new calibration files for the BCN and VAL instruments.

function) where possible using the effective wavelength of the channel rather than the nominal wavelength. Also for simplicity a unique daily value of column ozone, provided by GOME, was used. Brewer measurements were not used as they were available only for Armilla site, and usually for the used spectral windows the differences between Brewer and GOME values do not lead to considerable differences in AOD. For the calculation of the optical depth of water vapor and NO_2 we adopted the SMARTS 2.8 model algorithm [*Gueymard*, 2001]. For the content of each gas we considered the MLS (Middle Latitude Summer) standard values, corrected by height. This input showed to be better than columnar water vapor contents estimated from RH measurements. No independent measurements of NO_2 content were available, but the area is not polluted. Again, the absorption coefficients of water vapor and NO_2 were convoluted for the transmissivity profiles of each channel. In each case an assumed profile based on a Gaussian centered on the effective wavelength, with half width taken from the nominal filter bandpass, was used.

[40] In Figure 8 we show the compared behavior of the AOD, obtained with a common methodology and calibration source, during the intercomparison phase of the field campaign. In Table 12 the new deviations are presented. As can be seen in this table, the deviations between the different instruments decreased considerably compared to Table 12, and therefore we can confidently attempt to compare AOD for the instruments when deployed at the different sites for the field campaign, with a deviation in the retrievals that is well within the uncertainty.

[41] However, the deviation in Table 12 should not be understood as an improvement on the retrievals, as compared to results from Table 11, but rather it points out only minimized differences. It will be useful for later analyzing the atmospheric differences between the sites. In Figure 8 the error bars are not presented for clarity purposes although they were obtained again by the use of the error propagation method. The AOD maximum uncertainty computed in this way is very consistent with the nominal value 0.01–0.02 from *Eck et al.* [1999], although variable with the airmass during the day. This uncertainty is obviously dependent on the uncertainty of the calibration and the estimated uncertainty of the employed methodologies and input values. For AOD, it can be seen how the deviation was higher for the GFAT2 instrument. This deviation was maximum for 340 nm, related to a problem with the filter and the pointing system. These data have not been used for the analysis of the campaign, at least without a manual quality screening.

6. Intercomparison Licor-Cimel for AOD Measurements

[42] The comparison Licor-Cimel is only possible from the values of AOD. The AOD with the Licor 1800 was determined from the spectral irradiance measurements at normal incidence using the Bouger-Lambert-Beer exponential law, by following a series of steps which have been described by the authors in previous works [see, e.g., *Martínez-Lozano et al.*, 2001; *Pedrós et al.*, 2003]. We can summarize these steps by noting that the total optical depth can be expressed as the sum of the optical depths related to the different atmospheric components:

$$\tau_{T\lambda} = \tau_{R\lambda} + \tau_{a\lambda} + \tau_{O\lambda} + \tau_{w\lambda} + \tau_{N\lambda} \quad (5)$$

Table 10. Main Differences in the Preliminary Methodology Employed for AOD Retrieval With Cimel Instruments

	GOA	GRSV	CGE	GFAT (1 and 2)
Calibration source	VELETA Langley	VELETA Langley	VELETA Langley	VELETA Master
Air mass	Plane parallel	*Kasten and Young* [1989]	Plane parallel	*Gueymard* [2001]
Rayleigh scattering	*Gueymard* [2001]	*Bodhaine* [1999]	*Hansen and Travis* [1974]	*Gueymard* [2001]
Ozone content	TOMS	Microtops II	TOMS	Sounding (corrected)
Water absorption	None	*Gueymard* [2001]	None	None
NO2 absorption	None	*Gueymard* [2001]	None	*Gueymard* [2001]
Solar position	*Iqbal* [1983]	*Blanco-Muriel et al.* [2001]	*Iqbal* [1983]	*Blanco-Muriel et al.* [2001]
Refraction correction	None	*Michalsky* [1998]	None	None

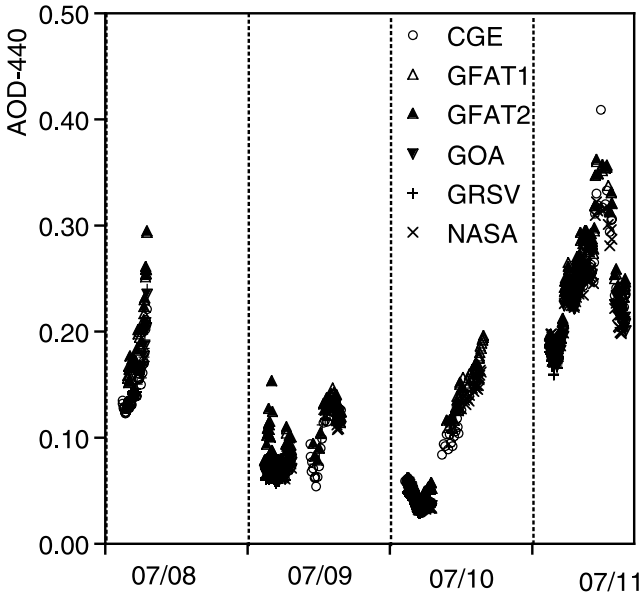

Figure 7. Comparison of the evolution of AOD during the intercomparison, obtained with independent methodologies for the different instruments.

where $\tau_{R\lambda}$ is the molecular scattering optical depth (which is usually calculated using the Rayleigh approximation), $\tau_{a\lambda}$ is the aerosol extinction optical depth, and $\tau_{O\lambda}$, $\tau_{w\lambda}$ and $\tau_{N\lambda}$ are the optical depths due to O_3, H_2O and NO_2 absorption, respectively. The absorption due to NO_2 has not been considered due to the rural character of the measurement site, leaving equation (5) as follows:

$$\tau_{T\lambda} = \tau_{R\lambda} + \tau_{a\lambda} + \tau_{O\lambda} \quad (6)$$

To determine $\tau_{T\lambda}$ we employed the values of the extraterrestrial spectrum proposed by the SMARTS2 model [*Gueymard*, 2001], smoothing the data to the band pass of our spectroradiometer. For the air mass, the empirical expression proposed by *Kasten and Young* [1989] was used. The Rayleigh optical depth was calculated from the approximation of *Bodhaine et al.* [1999], and the ozone absorption coefficients from *Anderson and Mauersberger* [1992] were assumed.

[43] Error propagation methods were applied to obtain the AOD error. *Utrillas* [1995] developed a simplified method to estimate the error associated with the AOD values retrieved from spectral irradiance measurements. This method is similar to that developed by *Russell et al.* [1993] and *Schmid et al.* [1997]. In our case the error in the AOD is mainly conditioned by the error in the measurement of the direct spectral irradiance and the value of the optical air mass at the instant of the measurement. The authors have previously used this method with experimental measurements made at other sites, and the values that were obtained were similar to those presented by *Kaufman et al* [1994].

[44] The results of the intercomparisons of the Licor-Cimel AOD measurements are presented below. The wavelengths used for this intercomparison were those corresponding to the Cimel central wavelengths, after convoluting the Licor irradiance measurements to match the

Table 11. Deviation (RMSD, MBD and STD) Calculated Between GFAT1 Instrument, and GRSV, AERONET, CGE, GFAT2, and GOA Instruments for AOD (n: Number of Points Analyzed)

λ, nm	RMSD	MBD	STD
	GRSV, n = 165		
440	0.019	0.018	0.008
670	0.013	0.011	0.007
870	0.011	0.008	0.007
1020	0.012	0.009	0.008
	AERONET, n = 196		
340	0.019	−0.007	0.018
380	0.022	0.015	0.016
440	0.019	0.016	0.010
670	0.017	0.016	0.004
870	0.012	0.011	0.007
1020	0.014	0.011	0.010
	CGE, n = 170		
440	0.020	0.016	0.012
670	0.008	−0.001	0.008
870	0.013	0.011	0.007
1020	0.014	0.012	0.007
	GFAT2, n = 181		
340	0.71	0.69	0.15
380	0.012	−0.003	0.012
440	0.010	−0.002	0.010
670	0.010	−0.001	0.010
870	0.007	−0.002	0.007
1020	0.014	−0.003	0.014
	GOA, n = 111		
440	0.019	0.018	0.008
670	0.011	0.009	0.007
870	0.011	0.008	0.007
1020	0.015	0.010	0.011

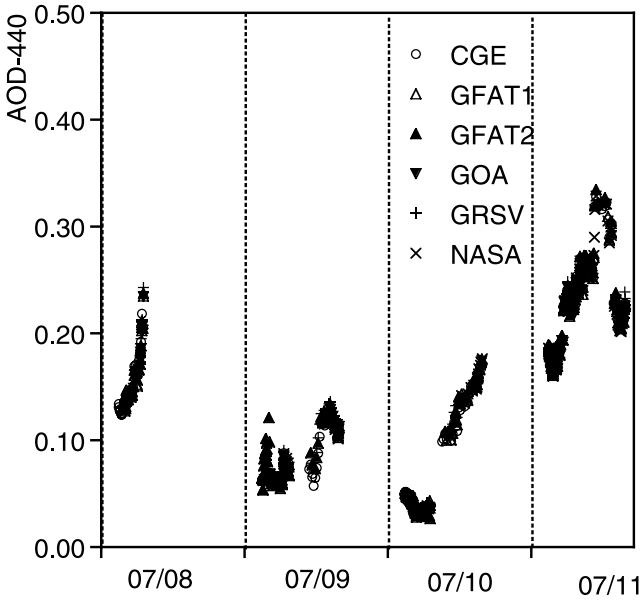

Figure 8. Comparison of the evolution of AOD during the intercomparison, obtained with a common methodology and calibration source.

Table 12. Deviation (RMSD, MBD, and STD) Calculated Between GFAT1 Instrument, and GRSV, AERONET, CGE, GFAT2, and GOA Instruments for AOD When the Common Methodology Was Applied (n: Number of Points Analyzed)

λ, nm	RMSD	MBD	STD
	GRSV, n = 165		
440	0.004	−0.002	0.003
670	0.005	−0.003	0.003
870	0.003	−0.002	0.003
1020	0.005	0.002	0.005
	AERONET, n = 196		
340	0.009	0.008	0.005
380	0.008	0.007	0.004
440	0.003	0.000	0.003
670	0.008	−0.006	0.005
870	0.004	−0.001	0.003
1020	0.006	0.001	0.006
	CGE, n = 170		
440	0.004	−0.002	0.004
670	0.004	−0.003	0.003
870	0.004	−0.002	0.003
1020	0.005	−0.001	0.005
	GFAT2, n = 181		
340	0.24	0.024	0.24
380	0.010	−0.001	0.010
440	0.009	−0.003	0.008
670	0.011	−0.007	0.009
870	0.007	−0.003	0.006
1020	0.012	−0.003	0.012
	GOA, n = 111		
440	0.003	0.002	0.003
670	0.005	−0.002	0.004
870	0.002	−0.000	0.002
1020	0.008	0.003	0.007

Cimel filter bandpasses. This can be only performed when the Cimel bandpass (2–10 nm depending on channel) is wider than the Licor bandpass (6 nm) that happens for the VIS and NIR channels. In any case the convolution represents a negligible variation on the direct irradiance measurements (0.2% for 870 nm, less than 0.1% for the other wavelengths). The effect of not matched bandwidths can be more important on the UV range. However, the Cimel for these channels has a narrower bandwidth than Licor and the effect cannot be accounted for. The results corresponding to 10 and 11 July when all the instruments were measuring at the Armilla site (first phase of the campaign) are presented first. Second, the results during the second phase of the campaign, corresponding to each measurement station, are given.

6.1. Intercomparison at Armilla

[45] During the first phase of the campaign, all the Licor and Cimel instruments were located at the same station, Armilla. Therefore we can compare all of the instruments together. In Table 13 the statistical deviations for the AOD values obtained from all the LiCor and Cimel measurements are presented. The AOD at 1020 nm showed an appreciable deviation. Given that the Licor detector is a Si photodiode, it presents an appreciable temperature dependence which, as it was not corrected for, could explain the larger deviations. In this campaign, however, the Licors were only used for studying the AOD in the visible range so such discrepancies at 1020 nm are of no importance. Therefore the results for 1020 channel have not been included in the analysis.

[46] As can be observed in Table 13, for the 340 nm channel the deviation was above the nominal uncertainty. This deviation is attributable to both instruments, Cimel and Licor. On the one hand, the Cimel has its maximum uncertainty at this wavelength, especially when we take into account the discrepancies found in the AERONET calibration and the calibration performed during this campaign. On the other hand, the Licor instrument at this wavelength is at the limit of the accuracy estimated for the visible range (5%). Therefore such a discrepancy was to be expected and was not important when we came to analyze the results since we only used the visible range for the Licor. In the case of the Cimel only three instruments (NASA, GFAT1, and GFAT2) measured in this channel so its usefulness was limited. In reality at Armilla the Cimel GFAT2 possessed a 340 nm channel but as we saw before its operation was completely defective.

6.2. Intercomparison at the Stations During the Second Phase of the Campaign

[47] The measurements used corresponded to the second phase of the campaign at the different stations (Motril, Pitres, Las Sabinas, and Armilla). At the Pico Veleta (3398 m a.s.l.) station no measurements were made as the strong winds prevented the automatic solar alignment of the Cimel from working correctly.

[48] To calculate the deviation it was considered that the instruments measured simultaneously when the readings were taken within 5 min of each other. This time interval was greater than used in the Cimel–Cimel (1 min) comparison since the synchronization (based on Local Apparent Time, LAT) in this case was much better for automatic measurement instruments. Given that the Licors were manually pointed, following a schedule based on GMT time every 15 min, this time difference was a nominal compromise value in order to take the maximum number of coincident measurements possible without suffering important appreciable time variations in the aerosol load during that time.

[49] As examples, Figures 9 and 10 show the evolution of the AOD corresponding to the 440 nm wavelength for all the measurement stations and all the measurement days as determined by the Licor 1800s and the Cimel CE318s, respectively. These figures show some characteristics of the aerosol load that, although not the objective of this work, are worth highlighting. For example the presence of fog at the Motril station on 13 and 14 July or the intrusion of Saharian dust beginning the afternoon of the 17 July seen

Table 13. Deviation (RMSD, MBD, and STD) Between AOD Mean Values Measured With all the Licor and all the Cimel[a]

Canal, nm	MBD	RMSD	STD
340	0.024	0.024	0.019
380	0.006	0.011	0.016
440	−0.001	0.006	0.011
670	0.011	0.011	0.009
870	0.016	0.016	0.009

[a]Armilla intercomparison phase.

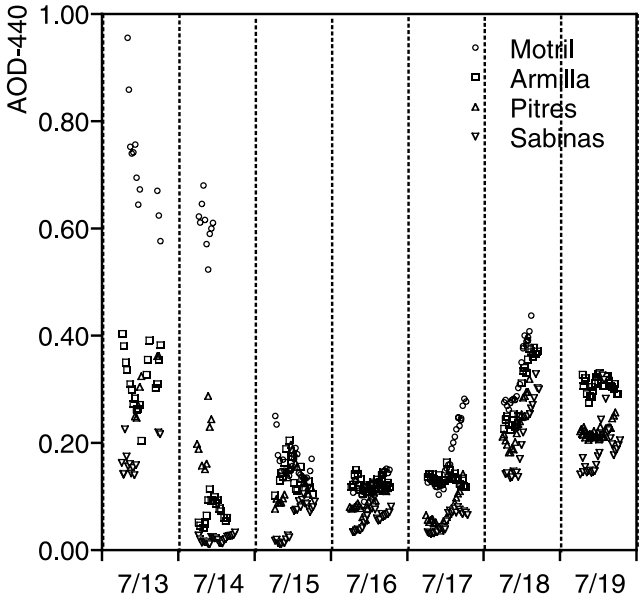

Figure 9. AOD for 440 nm determined by the Licor 1800s, for all the stations and all the days of the second phase of the measurement campaign.

first at Motril (on the south side of the Sierra Nevada) and later on the 18 July at the other measurement stations.

[50] Table 14 gives the deviations for each of the stations and for each measurement wavelength. From this table can be seen once again that the deviations between optical depth using the Cimels and the Licors in the visible range was around 0.01–0.03, depending on the channel and the meteorological conditions at the station. In all cases these deviations continued to be within the Licor uncertainty, ranging between 0.02 and 0.05, although they were occasionally above the nominal errors of the Cimel at 0.01–0.02.

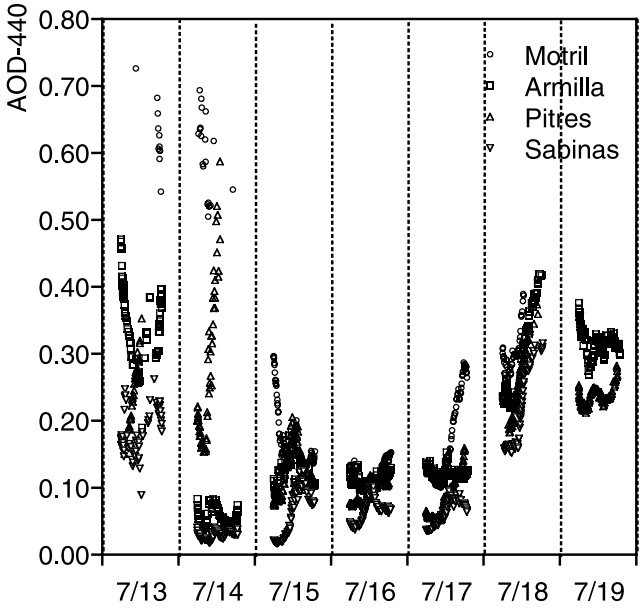

Figure 10. AOD for 440 nm determined by the Cimel 318s, for all the stations and all the days of the second phase of the measurement campaign.

7. Conclusions

[51] In relation to the Langley calibration of the Licor 1800s the constant values obtained for each of the spectroradiometers have been analyzed and the results showed that for the visible spectrum it was possible to reproduce in all cases the extraterrestrial irradiance within the range of experimental errors.

[52] The intercomparison of the Licor spectroradiometers, both for direct and global irradiance measurements, showed that when the entire spectral band was used the errors (average MAD in %) were almost all less than the instrument error. If the values were restricted to the visible range the errors between them were even less. These results for the behavior of the Licor-1800s used in the VELETA-2002 campaign allow us to affirm, by different methods, the suitability of these instruments for use at different measurement stations to obtain the physical properties of aerosols.

[53] A simultaneous calibration on AOD data was undertaken for the Cimel-318 Sun photometers, in order to assess their uncertainty and validity. Preliminary results with independent calibration and methodologies for each instrument showed that acceptable results could be achieved when compared with a field AERONET instrument, with a deviation mostly below 0.02 for AOD. However, if aerosol properties need to be compared between different sites at different heights, the deviation should be reduced in order to better identify the differences due only to aerosols, and not to instrumentation or methodology. Once this common calibration and methodology was applied, the deviation diminished to much less than 0.01 for AOD, also

Table 14. Average Deviations (in RMSD) for Each Measurement Station and for Each Selected Wavelength[a]

Canal, nm	RMSD	MBD	STD
Motril. Cimel GRSV-Licor GRSV, n = 86			
440	0.011	0.000	0.011
670	0.021	−0.018	0.013
870	0.027	−0.024	0.012
Armilla. Cimel CGE- Licor REPSOL, n = 133			
440	0.015	−0.009	0.012
670	0.014	−0.011	0.009
870	0.013	−0.010	0.009
Pitres. Cimel NASA-Licor GOA, n = 128			
340	0.099	−0.093	0.033
380	0.033	−0.030	0.013
440	0.016	0.010	0.026
500	0.011	0.003	0.010
670	0.010	0.001	0.019
870	0.018	−0.016	0.008
Las Sabinas. Cimel UGR1-Licor UGR, n = 118			
340	0.024	−0.021	0.012
380	0.013	0.007	0.022
440	0.013	0.011	0.019
670	0.005	0.003	0.009
870	0.009	−0.007	0.005

[a]Measurements were considered simultaneous when they differed by less than 5 min (n: number of points analyzed).

compared with AERONET values, and was well within the uncertainty of the measurements.

[54] An intercomparison was made between the AOD values provided by the spectroradiometers and by the Sun photometers giving a deviation between the results obtained for the optical depth using the Cimels and the Licors in the visible range from 0.01–0.03, depending on the channel and the meteorological conditions at each station. In some instance the deviation was above the nominal uncertainty of the Cimel (0.01–0.02) although always within the nominal uncertainty of the Licor (0.02–0.05).

[55] On the UVA range, from the estimated uncertainty on the calibration values of Cimel and Licor channels, we estimated the largest uncertainty on AOD (0.02 and 0.05 for Cimel and Licor respectively at 340 nm). These values were in agreement with the differences found in the Cimel–Cimel and Cimel–Licor comparisons, except for the GOA Licor (due to its optical probe) and the GFAT2 Cimel at 340 nm (due to a defective filter).

[56] Finally, it must be pointed out that as one of the objectives of the field campaign is "to obtain experimental data about the effects of atmospheric aerosols on solar ultraviolet irradiance," its usefulness will be limited at the UVA spectral range, due to instrumental uncertainties on the determination of the aerosol optical depth in the UVB spectral range.

[57] **Acknowledgments.** This work was financed by CICYT-MCYT through the Coordinated Project CLI2000-0903. V. Estellés, A. Alcántara, and A.M. Díaz currently hold research grants from the CICYT. Thanks to the MADOC, at the Base Aérea de Armilla, the Parque Nacional de Sierra Nevada, and the Ayuntamientos de Pitres and Motril for the support given throughout the campaign. We also would like to acknowledge B. Holben and other AERONET people for the 109 instrument and its data availability.

References

Alados-Arboledas, L., et al. (2003), VELETA 2002 field campaign, *Geophys. Res. Abstr.*, *5*, 12,218.

Alcántara, A., F. J. Olmo, and L. Alados-Arboledas (2004), Langley calibrations of sunphotometer at Sierra Nevada, Granada, Spain, *Opt. Pura Apl.*, *37*, 3263.

Anderson, S. M., and K. Mauersberger (1992), Measurements of ozone absorption cross section in the Chappuis band, *Geophys. Res. Lett.*, *19*, 933.

Blanco-Muriel, M., D. C. Alarcón-Padilla, T. López-Moratalla, and M. Lara-Coira (2001), Computing the solar vector, *Solar Energy*, *70*, 431.

Bodhaine, B. A., N. B. Wood, E. G. Dutton, and J. R. Slusser (1999), On Rayleigh optical depth calculations, *J. Atmos. Oceanic Technol.*, *16*, 1854.

Cachorro, V. E., M. P. Utrillas, R. Vergaz, P. Durán, A. de Frutos, and J. A. Martínez-Lozano (1998), Determination of the atmospheric water-vapor content in the 940 nm absorption band by use of moderate spectral-resolution measurements of direct solar irradiance, *Appl. Opt.*, *37*, 4678.

Cachorro, V. E., C. Toledano, R. Vergaz, A. M. de Frutos, M. Sorribas, J. M. Vilaplana, and B. de la Morena (2004), The PHOTONS-AERONET sites in Spain. Calibration problems and KCICLO correction method, *Opt. Pura Apl.*, *37*, 3401.

Campanelli, M., T. Nakajima, and B. Olivieri (2004), Determination of the solar calibration constant for a Sun-sky radiometer: Proposal of an in-situ procedure, *Appl. Opt.*, *43*, 651.

Cannon, T. W. (1986), Spectral solar irradiance instrumentation and measurement techniques, *Solar Cells*, *18*, 233.

Dubovik, O., B. N. Holben, T. F. Eck, A. Smirnov, Y. J. Kaufman, M. King, D. Tanré, and I. Slutsker (2002), Variability of absorption and optical properties of key aerosol types observed in worldwide locations, *J. Atmos. Sci.*, *59*, 590.

Eck, T. F., B. N. Holben, J. S. Reid, O. Dubovik, N. T. O'Neill, I. Slutsker, and S. Kinne (1999), Wavelength dependence of the optical depth of biomass burning, urban and desert dust aerosols, *J. Geophys. Res.*, *104*, 31,333.

Gueymard, C. A. (2001), Parameterized transmittance model for direct beam and circumsolar spectral irradiance, *Solar Energy*, *71*, 325.

Holben, B. N., et al. (1998), AERONET - A Federated instrument network and data archive for aerosol characterization, *Remote Sens. Environ.*, *66*, 1.

Holben, B. N., et al. (2001), An emerging ground-based aerosol climatology: Aerosol optical depth from AERONET, *J. Geophys. Res.*, *106*, 12,067.

Houghton, J., et al. (Eds.) (2001), *Climate Change: The Sicientific Basis*, Cambridge Univ. Press, New York.

Iqbal, M. (1983), *An Introduction to Solar Radiation*, Springer, New York.

Kasten, F., and M. T. Young (1989), Revised optical air mass tables and approximation formula, *Appl. Opt.*, *28*, 4735.

Kaufman, Y. J., A. Gitelson, A. Karnieli, E. Ganor, R. S. Fraser, T. Nakajima, S. Mattoo, and B. N. Holben (1994), Size distribution and scattering phase function of aerosol particles retrieved from sky brightness measurements, *J. Geophys. Res.*, *99*, 10,341.

Kuester, M. A., K. J. Kurtis, and A. Reagan (2003), Automated statistical approach to Langley evaluation for a solar radiometer, *Appl. Opt.*, *42*, 4919.

Labajo, A., , E. Cuevas, and B. de la Morena (Eds.) (2004), The first Iberian UV-visible instruments intercomparison, final report, 114 pp., Inst. Nacional de Meteorol., Ministerio de Medio Ambiente, Barcelona, Spain.

Martínez-Lozano, J. A., M. P. Utrillas, F. Tena, R. Pedrós, J. Cañada, J. V. Boscá, and J. Lorente (2001), Aerosol optical characteristics from Summer Campaign in an Urban Coastal Mediterranean Area, *IEEE Trans. Geosci. Remote Sens.*, *39*, 1573.

Martínez-Lozano, J. A., et al. (2002), UV Index experimental values during the years 2000 and 2001 from the Spanish broadband UVB radiometric network, *Photochem. Photobiol.*, *76*, 181.

Martínez-Lozano, J. A., et al. (2003), Intercomparison of spectroradiometers for global and direct solar irradiance in the visible range, *J. Atmos. Ocean Technol.*, *20*, 997.

McArthur, L. J. B., D. H. Halliwell, O. J. Niebergall, N. T. O'Neill, J. R. Slusser, and C. Wehrli (2003), Field comparison of network Sun photometers, *J. Geophys. Res.*, *108*(D19), 4596, doi:10.1029/2002JD002964.

Michalsky, J. J. (1988), The Astronomical Almanac's algorithm for approximate solar position (1950–2050), *Solar Energy*, *40*, 227.

Mitchell, R. M., and B. W. Forgan (2003), Aerosol measurement in the Australian Outback: Intercomparison of Sun photometers, *J. Atmos. Oceanic Technol.*, *20*, 54.

Morys, M., F. M. Mims III, S. Hagerup, S. E. Anderson, A. Baker, J. Kia, and T. Walkup (2001), Design, calibration and performance of MICROTOPS II handheld ozone monitor and Sun photometer, *J. Geophys. Res.*, *106*, 14,573.

Nann, S., and C. Riordan (1991), Solar spectral irradiance under clear and cloudy skies: Measurements and a semiempirical model, *J. Appl. Meteorol.*, *30*, 447.

Pedrós, R., J. A. Martinez-Lozano, M. P. Utrillas, J. L. Gómez-Amo, and F. Tena (2003), Column-integrated aerosol optical properties from ground-based spectroradiometer measurements at Barrax (Spain) during DAISEX (Digital Airborne Spectrometer Experiment) campaigns, *J. Geophys. Res.*, *108*(D18), 4571, doi:10.1029/2002JD003331.

Pietras, C., M. Miller, R. Frouin, T. Eck, B. Holben, and J. Marketon (2001), Calibration of Sun photometers and sky radiance sensors, in *In Situ Aerosol Optical Thickness Collected by the SIMBIOS Program (1997–2000): Protocols, and Data QC and Analysis*, *NASA/TM-2001-209982*, NASA, Washington, D. C.

Riordan, C., D. Myers, M. Rymes, M. Hulstrom, W. Marion, C. Jennings, and C. Whitaker (1989), Spectral solar radiation data base at SERI, *Solar Energy*, *42*, 67.

Russell, P., et al. (1993), Pinatubo and pre-Pinatubo optical depth spectra: Mauna Loa measurements, comparisons inferred particle size distributions, radiative effects, and relationships to lidar data, *J. Geophys. Res.*, *98*, 22,969.

Shaw, G. E. (1983), Sun photometry, *Bull. Am. Meteorol. Soc.*, *64*, 4.

Schimid, B., and C. Wehrli (1995), Comaparison of Sun photometer calibration by use of the Lanley technique and the standard lamp, *Appl. Opt.*, *34*, 4500.

Schmid, B., C. Mätzler, A. Heimo, and N. Kämpfer (1997), Retrieval of optical depth and particle size distribution of tropospheric and stratospheric aerosols by means of sun photometry, *IEEE Trans. Geosci. Remote Sens.*, *35*, 172.

Schmid, J., R. Michalsky, M. Halthore, L. Beauharnois, J. Harrison, P. Livingston, P. Russell, B. Holben, T. Eck, and A. Smirnov (1999), Comparison of aerosol optical depth from four solar radiometers during the fall 1997 ARM intensive observation period, *Geophys. Res. Lett.*, *26*, 2725.

Slusser, J., J. Gibson, D. Bigelow, D. Kolinsky, P. Disterhoft, K. Lantz, and A. Beaubien (2000), Langley method of calibrating UV filter radiometers, *J. Geophys. Res.*, *105*, 4841.

Utrillas, M. P. (1995), Estudio de aerosoles a partir de medidas de irradiancia solar spectral (in Spanish), Ph.D. thesis, Valencia Univ., Valencia, Spain.

World Meteorological Organization (WMO) (1994), Report on the measurements if atmospheric turbidity in BAPMoN, *GAW Rep. 94*, Geneva.

L. Alados-Arboledas, A. Alcántara, and F. J. Olmo, Grupo de Física de la Atmósfera, Dpto. de Física Aplicada, Universidad de Granada, Fuentenueva s/n 18071, Granada, Spain.

V. Cachorro, Grupo de Óptica Atmosférica, Dpto. de Óptica y Física Aplicada, Universidad de Valladolid, Prado de la Magdalena, s/n, E-47071 Valladolid, Spain.

J. Cañada, Grupo de Radiación Solar, Universidad Politécnica de Valencia, Camino de Vera s/n, E-46022 Valencia, Spain.

A. M. Díaz and J. P. Díaz, Dpto. de Física Básica, Universidad de La Laguna, Avd. Astrofísico Fco. Sánchez s/n, E-38206, La Laguna, Spain.

X. de Cabo and J. Lorente, Dpt de Astronomía i Meteorología, Universitat de Barcelona, Martí i Franquès, 1, E-08028 Barcelona, Spain.

T. Elías, and A. M. Silva, Évora Geophysics Centre, University of Évora, Rua Romão Ramalho 59, 7000 671 Évora, Portugal.

V. Estellés, J. A. Martínez-Lozano, and M. P. Utrillas, Grupo de Radiación Solar, Universitat de València, Dr. Moliner, 50, E-46100 Burjassot, Spain. (jmartine@uv.es)

Y. García, Centro Tecnológico Repsol-YPF, Carretera Extremadura A5 Km 18, E-28931 Móstoles, Madrid, Spain.

H. Horvath, Experimental Physics Institute, University of Vienna, Boltzmanngasse 5, Vienna, A-1090, Austria.

A. Labajo, Instituto Nacional de Meteorología, Camino de las Moreras s/n, Ciudad Universitaria, E-28040 Madrid, Spain.

M. Pujadas, Dpto de Impacto Ambiental de la Energía, CIEMAT, Avd. Complutense, 22, E-28040 Madrid, Spain.

J. A. Rodrigues, Departamento de Física, Universidade do Algarve, Departamento de Fisica, Campus de Gambelas, 8005-139 Faro, Portugal.

M. Sorribas, Estacion de Sondeos Atmosféricos de El Arenosillo, INTA, Ctra. San Juan del Puerto- Matalascañas Km.33, E-21130 Mazagón, Huelva, Spain.